Frequency Characteristics of a Bubble Cluster in a Vibrated Liquid Column

Hiroyuki Hashimoto* and Seiichi Sudo†
Tohoku University, Sendai, Japan

The purpose of the present paper is to investigate experimentally the dynamic behavior of the bubble cluster in detail and to clarify the frequency characteristics of the cluster by a theoretical model based on an experimental observation. It is found that the input acceleration required for the inception of the cluster formation is expressed by a semiempirical equation. By using this equation, it is possible to estimate quantitatively the influences of the ambient pressure and the liquid height on the inception of the cluster. The influence of the geometrical form of the container on the resonant frequency of the cluster is clarified quantitatively. The numerical values obtained by the present theory agree relatively well with the experimental values in both water and glycerol. The frequency characteristics of the liquid sloshing accompanying the cluster are clarified by the present investigation.

Nomenclature

a = dimensionless parameter
B = bulk modulus
C = wave velocity
D = diameter of container
E = Young's modulus of container
E_m = kinetic energy
E_p = potential energy
f = frequency
G = dimensionless acceleration, $=\omega^2 X_0/g$
g = acceleration of gravity
H = liquid height
K = coefficient for incipient cluster
k = proportional constant
M = strength of source
n = polytropic index
P = pressure
$\bar{P}$ = dimensionless pressure, $=P/(\rho g H)$
ΔP = pressure change at incipient cluster
Q = flow rate
R = distance from bubble center
r = radius
t = time
V = velocity or volume
ΔV = volume change at incipient cluster
X_0 = amplitude of input displacement
x,y = axial and radial coordinates, respectively
z' = physical plane, $=x'+iy'$
ζ = complex plane, $=\xi+i\eta$
ξ,η = complex coordinate
ρ = liquid density
ϕ = dimensionless angular frequency, $=\omega H/C_s$
ψ = stream function
ω = angular frequency

Subscripts

a = ambient pressure or individual bubble
c = cluster or representative value at $t=0$
g = gas
i = incipient cluster
l = liquid or distance between free surface and cluster center
s = oscillating system
v = vapor
x,y = component x and y directions, respectively
0 = input value
$\bar{(\ )}$ = dimensionless relative to H
$(\ )'$ = dimensionless relative to D

Received July 13, 1984; revision received Oct. 27, 1984.

*Professor, Institute of High Speed Mechanics. Member AIAA.
†Research Assistant, Institute of High Speed Mechanics.

Introduction

LIQUID sloshing phenomena have been studied in connection with the dynamics of liquid-fuel rockets, chemical engineering processes, safety designs of oil reservoirs, nuclear reactors during earthquakes, etc. The disintegration of the liquid free surface and the gas entrainment[1] were observed frequently by increasing the input acceleration of a vertical oscillating container. As a result, gas bubbles may be formed in an oscillating liquid.

Regarding the motion of gas bubbles in vertically vibrated liquid columns, the mechanism of gas entrainment,[2] cyclic migration,[3] equilibrium position of a bubble in a vibrated liquid column,[4] viscous effect on the equilibrium position,[5] mutual attraction of bubbles,[6] and the coalescence of two bubbles[7] have been investigated. On the other hand, the small bubbles formed close to the free surface by the gas entrainment gather around a point and the large majority of bubbles sometimes make a cluster. Regarding the motion of the bubble cluster, pressure distribution,[8] threshold pressure required to produce bubble formation,[9] bubble coalescence,[10] surface instability,[11] and surface tension effect[12] have been investigated macroscopically.

However, there are a number of unclarified points regarding the dynamic behavior of the cluster. Especially the insufficient research data on the complicated frequency characteristics of the liquid sloshing accompanying a cluster. Further research into the frequency characteristics of the cluster in the oscillating liquid column would be helpful to understand the liquid sloshing phenomena.

The purpose of the present paper, therefore, is to investigate experimentally the dynamic behavior of a cluster in detail and to clarify the frequency characteristics of the cluster by a theoretical model based on an experimental observation. The basic frequency characteristics of liquid sloshing without the cluster have already been discussed in Ref. 13. In the present paper, a bubble cluster in a vertically oscillating cylindrical liquid column is investigated. An interesting conclusion is drawn by comparing the experimental results with the theoretical results for both the threshold acceleration required for the cluster formation and the resonant frequency of the cluster.

Experimental Apparatus

An experimental apparatus is shown in Fig. 1. An acrylic plastic cylinder, 500 mm long, 6 mm thick, and 119 mm in diameter containing water, was excited longitudinally and sinusoidally by an electrodynamic shaker (a few tests were conducted with a container 500 mm long, 8 mm thick, and 184 mm in diameter). The shaker was operated by a control system. The container motion was measured by an accelerometer monitored on a dual-trace oscilloscope and an electromagnetic oscillograph. The motions of the clusters were photographed by a high-beam stroboscope-streak camera system and a 16-mm high-speed movie camera. The photographs of the clusters were analyzed by a film motion analyzer.

Bubble Cluster Behavior

Bubble Cluster Formation

At a larger input acceleration than the specified value, the violent surface agitation made the many small gas bubbles close to the free surface in a degree hardly discernible, and they grew due to the large liquid pressure amplitude. The bubbles often became negatively buoyant during each oscillation period and thus sank toward the container bottom. The bubbles also attracted each other due to a mutual attraction between bubbles and gathered around a point. Such behavior is referred to as motion produced by Bjerknes' force.[2] The large majority of the gathering bubbles did not coalesce and formed a cluster. The cluster moved through the liquid column or remained at the specified position corresponding to the amount of the input acceleration. It was often observed that a few small clusters together with several isolated bubbles gathered around the center of the container bottom and grew into a few larger clusters over the wide range of the input acceleration.

Figure 2 shows the three representative patterns of the cluster formation for $H' = H/D = 2.5$ and $G_0 = 2\text{-}8$. Figures 2a-c show an unstable state before mutual attraction, a sufficiently developed stable state, and an unstable partially coalesced state, respectively. The developed cluster shown in Fig. 2b was composed of many individual small bubbles and pulsated as a whole. The geometrical form of the cluster was not always a sphere; sometimes it became a half-sphere or a circular disk when it remained at the bottom or the side wall of the container. When the input acceleration was gradually decreased, buoyancy forces became predominant and the cluster deformed like a vertically enlarged mushroom, as shown Fig. 2c, and sometimes coalesced into a single larger bubble or separated into a few large bubbles during its upward movement. When it reached the free surface, the gas of the cluster was discharged into the atmosphere. Generally, the cluster was divided into two parts. One was the outer region of the cluster where the distance between bubbles is relatively large, and the other was the inner region where the bubbles exist very close together.

Motions of Individual Bubble and Cluster

Figure 3 shows the motions of the center points of two bubbles that were forming a cluster based upon the mutual attraction between bubbles. The distance R from the temporary point to the bubble center was measured using a film motion analyzer with the high-speed movie films taken at 3000 frames/s. The individual bubbles approached each other. A small individual bubble (the radius is about 0.1-2.5 mm in the experiment) in a cluster expanded and was compressed cyclically with a small amplitude for a given input condition. Figure 4 shows the representative example of the radius of an individual bubble in a cluster for an input period. The experimental results were obtained with the high-speed movie camera. The theoretical curve was obtained from

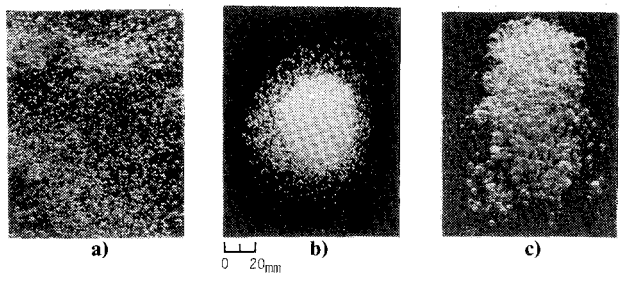

Fig. 2 Representative patterns of a cluster.

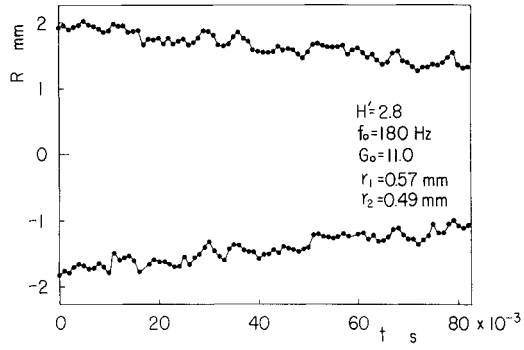

Fig. 3 Individual bubble approach by mutual attraction.

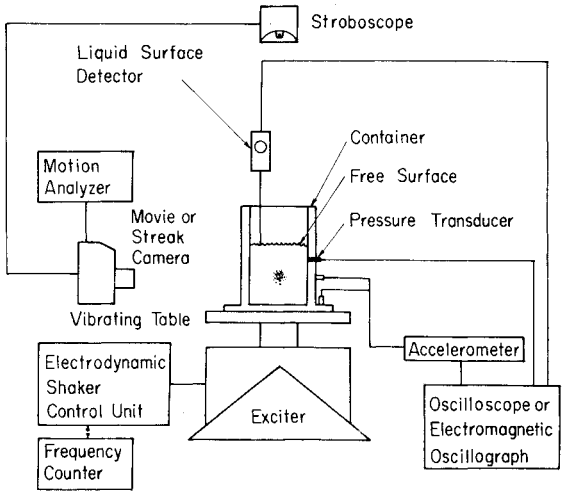

Fig. 1 Experimental apparatus.

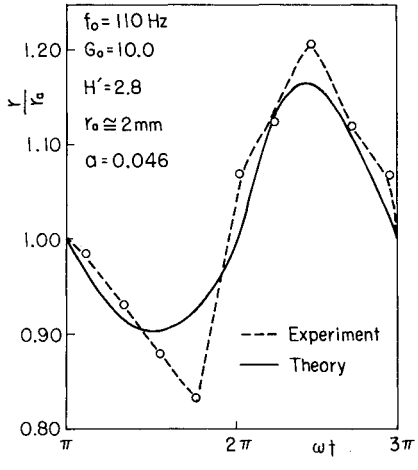

Fig. 4 Radius-time curve for an individual bubble in a cluster.

the ideal model under the assumption that a single spherical bubble oscillated in the following pressure field and bubble radius[2]:

$$\bar{P}-\bar{P}_a=\bar{x}+a\sin(\omega t),\quad r'=r'_a\{1+a\sin(\omega t)\}^m \tag{1a}$$

$$\bar{P}=\frac{P}{\rho_l g H},\quad \bar{x}=x'\frac{D}{H},\quad a=\frac{-G\sin(\phi\bar{x})}{\phi(\bar{P}_a+\bar{x})\cos\phi} \tag{1b}$$

$$m=\frac{1}{3n},\quad \phi=\frac{\omega H}{C_s},\quad G=\frac{\omega^2 X_0}{g},\quad r'=\frac{r}{D},\quad x'=\frac{x}{D} \tag{1c}$$

The individual bubble in the cluster pulsated from the theoretical curve more violently and steeply than expected. The difference between the theory and experiment seemed to be caused by the strong radial fluctuation of the individual bubbles themselves around the center of the cluster as described below.

Figure 5 shows the pulsating motion of a cluster. The diameters $2r_{cx}$ and $2r_{cy}$ were defined as the maximum linear distance between two opposite points on the outermost boundary of the cluster in the direction of the x and y coordinates, respectively. Two lines, r_{cx} and r_{cy}, intersect at right angles. These diameters were measured with high-speed movie films. It is seen that the cluster pulsates as a whole as if a single large bubble having the same radius as the outermost cluster boundary pulsates and that the pattern of the boundary changing with time was very steep and also relatively regular. Figure 6 shows the relation of the input frequency to the mean cluster frequency obtained from Fig. 5. From the figure, it is seen that the cluster frequency agrees approximately with the input frequency and that it is independent of the liquid depth in the container.

Threshold Acceleration for Incipient Cluster

The experimental observation revealed the following: 1) the higher the input frequency, the faster and more easily the bubbles gathered around the point (the velocity of the moving bubbles due to the Bjerknes' force increased with the input frequency[2]), and 2) the larger the void fraction became due to the air entrainment, the more easily the cluster was formed. For convenience, assuming that the bulk moduli of the liquid and the gas are $B_l=\infty$ and $B_g=0$, respectively, the volume change ΔV_s of the two-phase mixture produced by the pressure change equals the total volume V_g of the gas entrainment ($\Delta V_g=V_g$, $\Delta V_l=0$). Therefore, the volumetric strain $(\Delta V/V)_s$ of the oscillating system equals the void fraction $V_g/(V_g+V_l)$ of the system. The relation of $(\Delta V/V)_s$ to the pressure amplitude ΔP of the liquid is approximately expressed as follows[9]:

$$\left(\frac{\Delta V}{V}\right)_s=\left(\frac{\Delta P}{C^2\rho}\right)_s\cong\frac{\Delta P}{C_s^2\rho} \tag{2}$$

By using the fluid bulk modulus B and thickness S of the container wall, the wave velocity C_s is expressed as

$$C_s\cong\sqrt{\frac{B}{\rho\{1+(DB/SE)\}}}\cong\sqrt{\frac{SE}{\rho D}} \tag{3}$$

If the condition $G>1$ is satisfied in Eqs. (1), the minimum pressure of the system is obtained at $\bar{x}=1$ (the container bottom) for $0\le\phi\le\pi/2$, and at $\bar{x}=\pi/(2\phi)$ for $\phi>\pi/2$ when $(\cos\phi)/G\cong 0$. Therefore, the pressure amplitude $\Delta P/(\rho g H)$ is expressed as follows:

$$\frac{\Delta P}{\rho g H}=\frac{G\tan\phi}{\phi}\quad \text{for } 0\le\phi\le\pi/2 \tag{4a}$$

$$=\frac{G}{\phi\,|\cos\phi|}\quad \text{for } \phi>\pi/2 \tag{4b}$$

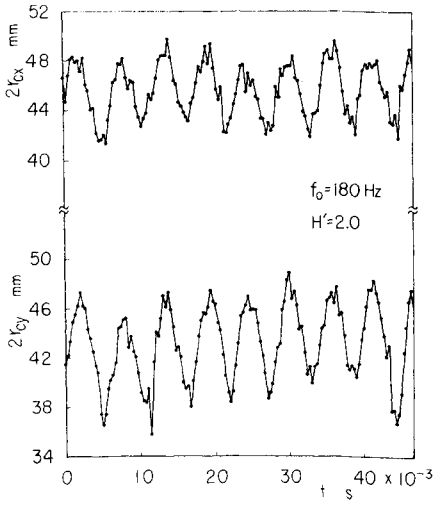

Fig. 5 Pulsating motion of a cluster.

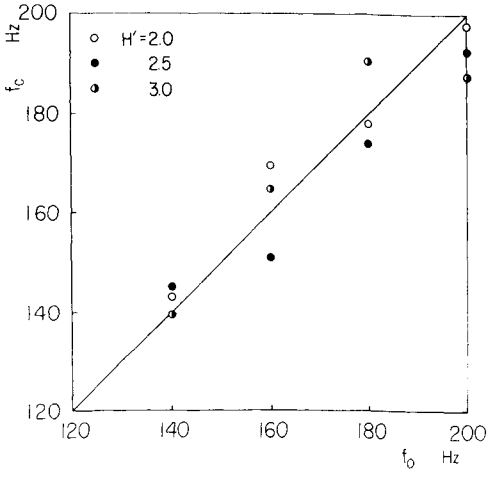

Fig. 6 Relation of cluster frequency to input frequency.

Considering the air entrainment and the bubble formation process, the pressure P_i of the individual bubble in the incipient cluster formation confirmed with the naked eye is assumed to be as follows:

$$P_i=P_v+K(P_a-P_v) \tag{5}$$

The coefficient K is taken to be the value from 0 to 1 ($P_v\le P_i\le P_a$), and K seems to be approximately in proportion to $(\Delta V/V)_s$ and the input frequency f_0, as described previously. Finally, the incipient condition of the cluster is obtained by using Eqs. (2-5) as follows:

$$K=k\left(\frac{\Delta V}{V}\right)_s\left(2\pi f_0\sqrt{\frac{D}{g}}\right)$$

$$=\sqrt{gD}\,kG\sqrt{\frac{D\rho}{SE}}\tan\phi\quad \text{for } 0\le\phi\le\pi/2 \tag{6a}$$

$$=\sqrt{gD}\,kG\sqrt{\frac{D\rho}{SE}\frac{1}{|\cos\phi|}}\quad \text{for } \phi>\pi/2 \tag{6b}$$

Here k is the proportional constant.

If the container was oscillated near the pressure resonant frequency $\phi=\pi/2$, many bubbles produced near the free surface by the gas entrainment moved smoothly and rapidly to the bottom of the container and remained there, and the

scale of each bubble did not change. In this case, the pressure in the bubble seemed to approach the atmospheric pressure, i.e., $K \cong 1$. For instance, such a state was observed under the input conditions $H/D=2.5$, $\phi=1.47$, and $G=7.2$. Substituting these values and $\bar{x}=1$ and K into Eqs. (6), the constant k equals approximately $10\pi/(\sqrt{gH})$. From Eqs. (4-6) and $\bar{P}_i-\bar{P}_a=\bar{x}-\Delta P/(\rho gH)$, the following threshold acceleration G_i required for the inception of the cluster is obtained:

$$G_i=\frac{\{(\pi/2)+(\bar{P}_a-\bar{P}_v)\phi\}(\cos\phi)}{1+5\phi(\bar{P}_a-\bar{P}_v)\sqrt{D\rho_l/(SE)}} \quad \text{for } 0\leq\phi\leq\pi/2 \qquad (7a)$$

$$=\frac{\{1+(\bar{P}_a-\bar{P}_s)\phi\}(\phi/\tan\phi)}{1+5\phi(\bar{P}_a-\bar{P}_s)\sqrt{D\rho_l/(SE)}} \quad \text{for } \phi>\pi/2 \qquad (7b)$$

Figure 7 shows the relation of the threshold dimensionless acceleration G_i to ϕ. In the figure, the solid curve is obtained by Eqs. (7), and the dotted curve is the threshold of the cluster which is obtained by Schoenhals and Overcamp[9] on the assumption that the pressure of the liquid reduces to the vapor pressure of the liquid in the same way as the cavitation inception. The present theoretical curve agrees well with their experimental results for methanol.[9] From Fig. 7, it is seen that G_i decreases with increasing ϕ in the region $0<\phi<\pi/2$, while G_i increases with increasing ϕ in the region $\pi/2<\phi<\pi$.

Figure 8 shows the relation of G_i to the dimensionless ambient pressure $(\bar{P}_a-\bar{P}_v)$ of water. The theoretical results obtained from Eqs. (7) agree approximately with the present experimental results at the atmospheric pressure. If ϕ is held to be constant, the threshold acceleration G_i increases smoothly with the dimensionless parameter $(\bar{P}_a-\bar{P}_v)$.

Response of Container Wall

The radial acceleration of the container wall has a maximum at the pressure resonant values of the system obtained from Eqs. (1): $\phi=\pi/2$, $3\pi/2$,. . . The cluster was easily formed at these resonant frequencies which lowered as H' became larger. Figure 9 shows the radial acceleration distribution along an axial line of the container with water height $H'=2.0$. The dimensionless acceleration G_w was measured on the outer surface of the container wall. When the input frequencies f_0 and H' were held to be constant, G_w increased with an increase of the input acceleration G_0. The wall acceleration after the cluster formation showed a very different response from the oscillating mode prior to the cluster formation, as shown in the figure. The wall response with the cluster was violently disturbed and showed a large swell with a much longer period than $1/f_0$. Such a tendency after the cluster formation changed only slightly for varying H'. This means that the frequency characteristics of the oscillating system depend strongly on the existence of the bubble cluster.

The radial acceleration of the wall seemed to be closely related with the liquid pressure. Of course, the remarkable, large radial acceleration of the wall occurred in the vicinity of the resonant frequency of the oscillating system concerned with the liquid pressure. The resonant frequencies of the system obtained by measuring the liquid pressure showed the values above 260 Hz for the present experimental region $G_0=2$-12 at $H'=2.5$. The detail of the liquid pressure is omitted in the present paper because both the liquid pressure and the resonant frequency without the cluster are discussed in Ref. 13.

Resonant Frequency of Cluster

Since it was necessary to clarify the frequency characteristics of the liquid sloshing accompanying a cluster, the resonant frequency of the cluster in the oscillating system

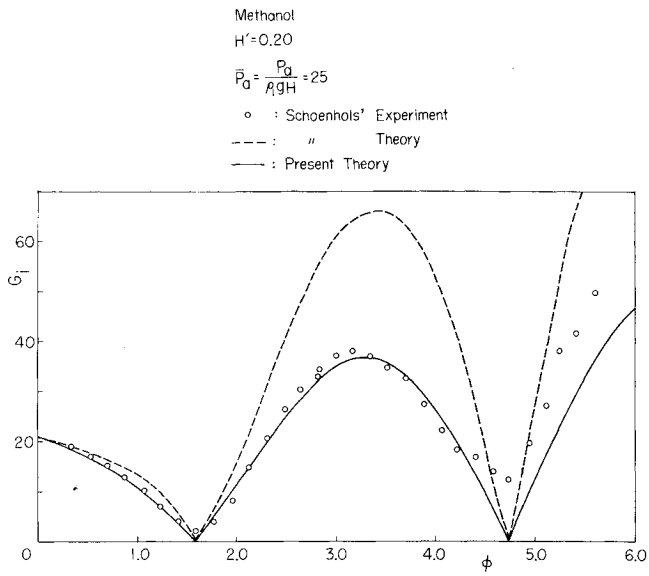

Fig. 7 Comparison of input acceleration between experiment and theory for incipient cluster.

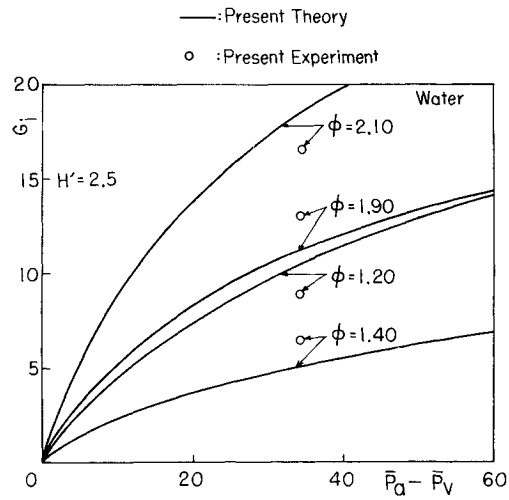

Fig. 8 Relation of input acceleration to dimensionless pressure $(\bar{P}_a-\bar{P}_v)$ for incipient cluster.

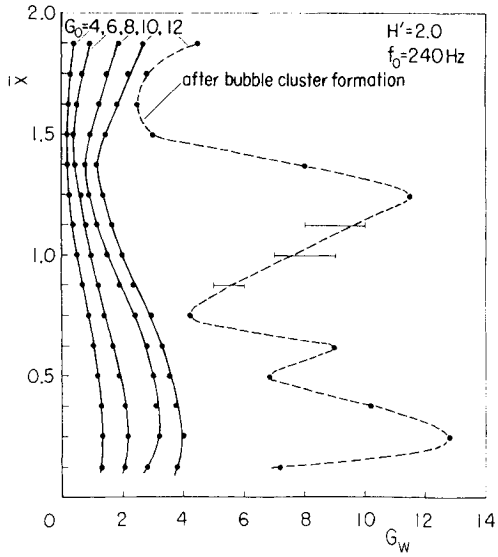

Fig. 9 Radial acceleration of container wall along axial line of container.

was analyzed by the conformal mapping method, based on the simple fluid model.

Stream Function and Strength of the Source

According to the experimental results, the following oscillating conditions are assumed.

1) The cluster is located on the center axis of the cylindrical container, and the fluid motion is axisymmetric. Both velocity potential and stream function can be used.

2) The cluster composed of the many individual bubbles, as described in Fig. 5, pulsates radially as a whole as if it is a single large spherical bubble; the temporary contour of the outermost individual bubbles in the cluster repeats the same compressive and expansive motion periodically as a large spherical bubble.

3) The periodic motion of the liquid based on the cluster pulsation is expressed equivalently by a source whose strength changes periodically.

By taking the inner diameter D of the container as the representative length, the physical plane ($z'=x'+iy'$) is mapped on the right half of the ζ plane ($\zeta=\xi+i\eta$), as shown in Fig. 10. With reference to the Schwarz-Christoffel transformation, the mapping function is expressed as

$$\zeta=\sinh\pi z' \tag{8}$$

A center point x_c' of the cluster on the z' plane is mapped on a point ζ_c on the ζ plane. By applying the image principle, the following stream function, satisfying the equation of continuity and the boundary condition, is obtained:

$$\begin{aligned}\psi=&\frac{M(\xi-\xi_c)}{\sqrt{(\xi-\xi_c)^2+\eta^2}}+\frac{M(\xi+\xi_c)}{\sqrt{(\xi+\xi_c)^2+\eta^2}}\\&=\{M(\sinh\pi x'\cos\pi y'-\sinh\pi x_c')\}\{\sinh^2\pi x'\\&+\sin^2\pi y'-2\sinh\pi x_c'\sinh\pi x'\cos\pi y'\\&+\sinh^2\pi x_c'\}^{-1/2}+\{M(\sinh\pi x'\cos\pi y'+\sinh\pi x_c')\}\\&\times\{\sinh^2\pi x'+\sin^2\pi y'+2\sinh\pi x_c'\sinh\pi x'\cos\pi y'\\&+\sinh^2\pi x_c'\}^{-1/2}\end{aligned} \tag{9}$$

The velocity components V_x and V_y are expressed as

$$V_y=-\frac{1}{y'}\frac{\partial\psi}{\partial x'},\quad V_x=\frac{1}{y'}\frac{\partial\psi}{\partial y'} \tag{10}$$

Figure 11 shows a representative example of the numerical results for the stream function and the velocity distribution in $x_c'=0.7$ and $r_c'=0.05$. In the figure, the scale of the arrow is in proportion to the amount of the velocity. The flow rate

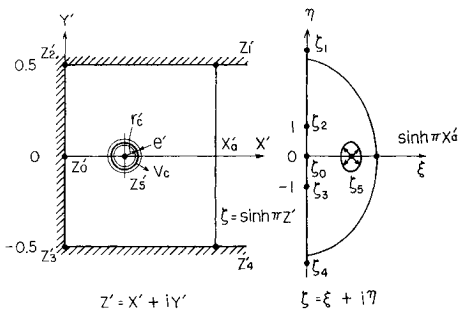

Fig. 10 Physical and conformal planes.

Q and the radial representative velocity V_c of the cluster boundary at $r=r_c$ are shown as follows:

$$Q=2\pi D^2\int_0^{1/2}y'V_x\mathrm{d}y'=2\pi D^2(\psi_{y'=1/2}-\psi_{y'=0})=-4\pi D^2M \tag{11}$$

$$V_c=\frac{Q}{4\pi r_c^2}=\frac{-D^2M}{r_c^2} \tag{12}$$

If the radius r of the outer boundary of the cluster is expressed in the same function as Eqs. (1) based on the assumption described above, the radius of the cluster for a given time is obtained as

$$r/r_c=(1+a\sin\omega_c t)^m \tag{13}$$

Here, r_c is the representative radius of the cluster at $t=0$. Since the maximum velocity $(\mathrm{d}r/\mathrm{d}t)_{\max}$ of the cluster boundary is equal to the representative velocity V_c, V_c is expressed approximately in Eq. (14) when $a<1$, i.e.,

$$V_c=[(1-a^2+ma^2\cos^2\omega_c t)^{m-1}\,r_cma\omega_c\cos\omega_c t]_{\max}\cong r_cma\omega_c \tag{14}$$

From Eqs. (12) and (14), the relation $M=r_c^3ma\omega_c/D$ is obtained.

Total Energy and Resonant Frequency

By dividing the liquid field into three specified regions (region I, $H'\geq x'\geq x_c'+r_c'$; II, $x_c'+r_c'\geq x'\geq x_c'-r_c'$; and III, $x_c'-r_c'\geq x'\geq 0$) as shown in Fig. 11, the total kinetic energy of the liquid is as follows:

$$\begin{aligned}E_m=&\frac{1}{2}\rho_l\int\int_{\text{liquid}}2\pi yV^2\mathrm{d}y\mathrm{d}x\\&=\pi\rho_lD^3\left\{\int_{x_c'+r_c'}^{H'}\int_0^{1/2}y'V^2\mathrm{d}y'\mathrm{d}x'\right.\\&+\int_{x_c'-r_c'}^{x_c'+r_c'}\int_{\sqrt{r_c'^2-(x'-x_c')^2}}^{1/2}y'V^2\mathrm{d}y'\mathrm{d}x'\\&\left.+\int_0^{x_c'-r_c'}\int_0^{1/2}y'V^2\mathrm{d}y'\mathrm{d}x'\right\}\end{aligned} \tag{15}$$

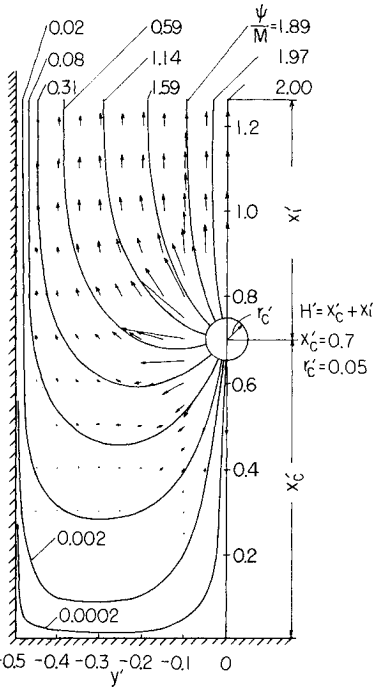

Fig. 11 Stream functions and velocity distributions.

By neglecting the small second-order terms for r_c' under the conditions $x_l' \gg r_c'$, $x_c' \gg r_c'$, and $1 \gg r_c'$, and using an approximating equation $(\sin\pi y')/(\pi y') \cong 3/4 + (1/4)\cos^2(\pi y')$, we obtain

$$E_m = 2\pi\rho_l m^2 a^2 r_c^5 \omega_c^2 \left[1 + \pi^2 r_c' \left(2.4x_l' + \frac{x_c'}{8} - 3.1r_c' - \frac{1.1}{\pi}\right)\right] \quad (16)$$

Even under the extreme condition $x_c' = 0$, the value E_m at $r_c' = 0.2$ in Eq. (16) agrees with the exact value obtained by locating the source on $x' = 0$ within a 15% error.

By considering $P/P_c = \{r_c^3/(r_c - e)^3\}^n$, the maximum potential energy E_p (at the minimum cluster volume) is expressed as follows:

$$E_p = \int_{V_{\min}}^{V_c} (P - P_c)\,dV = \int_0^{e_{\max}} (P - P_c)\frac{3n}{r_c}(4\pi r_c^2)de$$

$$= 4\pi r_c^3 P_c \frac{3n}{3n-1}\left\{\left(1 - \frac{a}{3n}\right)(1-a)^{-1/3n} - 1\right\} \quad (17)$$

Here, e is the displacement of the cluster boundary measured from the mean radius r_c, and the mean pressure P_c at $r = r_c$ $(t = 0)$ is equal to $P_a + \rho_l g x_l$.

The total kinetic energy must balance with the maximum potential energy, therefore, Eqs. (16) and (17) can be solved for $f_c = \omega_c/(2\pi)$ as follows:

$$\frac{f_c}{f_M} = \left[1 + \pi^2 r_c' \left(2.4x_l' + \frac{x_c'}{8} - 3.1r_c' - \frac{1.1}{\pi}\right)\right]^{-1/2} \quad (18)$$

Here, $f_M = \sqrt{3n(P_a/\rho_l + gx_l)}/(2\pi r_c) = \sqrt{3nP_c/\rho_l}/(2\pi r_c)$. If $P \to \infty$, Eq. (18) coincides with the simple equations obtained by Minnaert,[14] who introduced to the case that there exists a single bubble in the infinite liquid field. On the other hand, Baird[15] obtained a resonant frequency f_a of a single bubble on the assumptions that 1) the volume of liquid above the bubble undergoes piston-type pulsations, and 2) radial pulsations extend outward from the bubble surface to the spherical boundary. He also introduced the following equation by neglecting the influence of the container wall below the bubble:

$$f_a/f_M = [1 + 2r_a'(8x_l' - 1)]^{-1/2} \quad (19)$$

If x_c' and r_c' are much smaller than x_l', f_c in Eq. (18) agrees approximately with f_α in Eq. (19).

Figure 12 shows the numerical results of Eq. (18) at $H' = 2.5$ for water. From the figure, it is seen that the resonant frequency f_c of the cluster in the oscillating system is always lower than f_M, which coincides perfectly with the solution for the infinite field. And f_c/f_M decreases with an increase of both r_c' and x_l'. For instance, in the case $r_c' = 0.1$ and $H' = 2.5$, f_c is about half of f_M at $x_l' = 1.5$ and f_c is 0.40 f_M at $x_l' = 2.5$ (the cluster is located at the bottom). Figure 13 shows the comparison of the present experimental and theoretical results for the resonant frequency f_c at $H' = 2.5$, $x_l' = 1.66$ in the water. f_c decreases steeply with an increase of the cluster volume V_c, i.e., the cluster radius r_c. Two other theoretical curves for a bubble are also shown in the figure for reference. The difference between the present curve and Baird's curve[15] might be caused by neglecting the boundary condition on the wall below the bubble in Baird's theory. The present theory for the water agrees with the experimental values better than Baird's theory and Minnaert's theory as well. Figure 14 shows the relation of the resonant frequency f_c to the cluster radius r_c and the cluster location x_l inglycerol. From the figure, it is seen that f_c decreases with an increase in both r_c and x_l, and that f_c is influenced by r_c more strongly than x_l. The theoretical and experimental

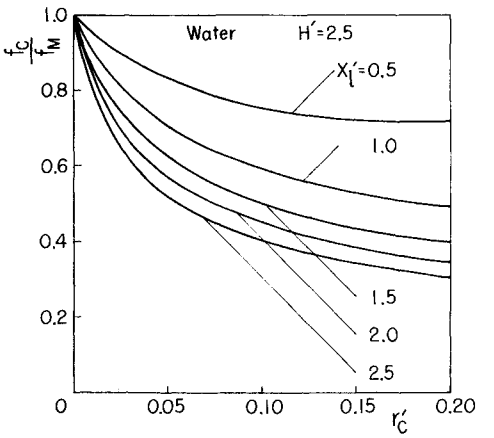

Fig. 12 Numerical results of resonant frequency for water.

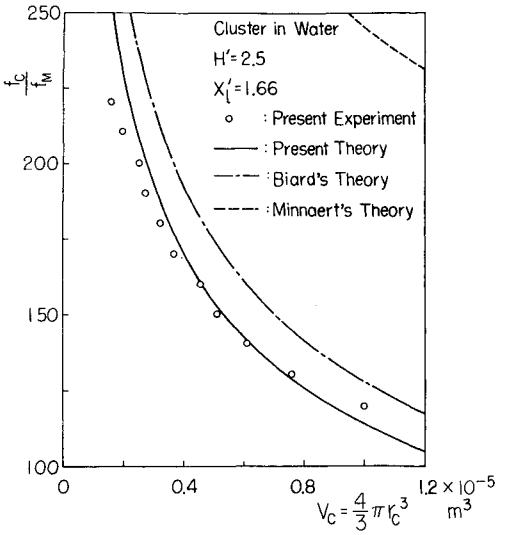

Fig. 13 Comparison of theoretical resonant frequency with experimental frequency for water.

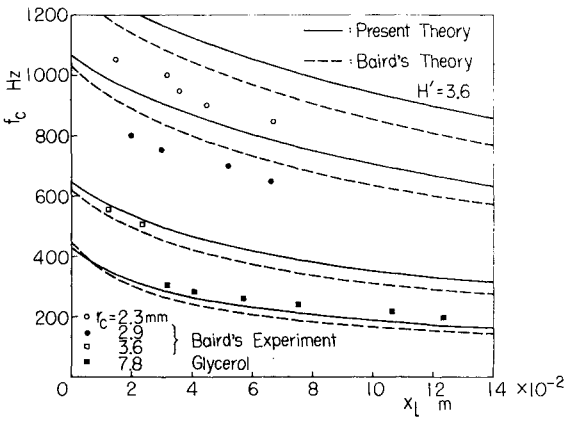

Fig. 14 Relation of resonant frequency to x_l for glycerol.

results of a bubble obtained by Baird[15] are also plotted in the figure for reference. The difference between the present theory and the experiment might be caused mainly by the unsuitable expression of the pressure field and the lack of consideration of the nonlinearity effect due to the liquid viscosity in the theory.

As shown in Figs. 12-14, the resonant frequency of a cluster in the cylindrical container with relatively high accuracy can be estimated by using Eq. (18). The analyses and numerical results for the cluster described previously

clarified the frequency characteristics of the liquid sloshing in greater detail.

Conclusions

1) The individual bubbles in the cluster pulsate with the same frequency as the input frequency of the container. The surfaces of the individual bubbles pulsate very violently and steeply. The cluster, as a whole, pulsates radially with the same frequency as the input frequency, as if only a single large spherical bubble were pulsating in the oscillating liquid column.

2) The input acceleration required for the inception of the cluster formation is expressed semiempirically in Eqs. (7). By using this equation, it is possible to estimate quantitatively the influences of the ambient pressure and liquid height on the inception of the pressure and the liquid height on the inception of the cluster.

3) The response of the container wall changes abruptly as soon as the cluster forms in the oscillating liquid column; the radial acceleration of the container wall becomes much larger and more complex than the wall response without the cluster.

4) The influence of the geometrical form of the container on the resonant frequency of the cluster was clarified quantitatively. The numerical values obtained by the present theory agreed relatively with the experimental values in both water and glycerol. The frequency characteristics of the liquid sloshing accompanying the cluster were clarified by the present investigation.

References

[1]Abramson, H. N., "The Dynamic Behavior of Liquids in Moving Containers," NASA-SP-106, 1966.

[2]Hashimoto, H. and Sudo, S., "Surface Disintegration and Bubble Formation in Vertically Vibrated Liquid Column," *AIAA Journal*, Vol. 18, April 1980, pp. 442-449.

[3]Buchanan, R. H., Jameson, G., and Oedjoe, D., "Cyclic Migration of Bubbles in Vertically Vibrating Liquid Columns," *Industrial and Engineering Chemistry Fundamentals,* Vol. 1, May 1962, pp. 82-86.

[4]Kana, D. D. and Dodge, F. T., "Bubble Behavior in Liquids Contained in Vertically Vibrated Tanks," *Journal of Spacecraft and Rockets,* Vol. 3, May 1966, pp. 760-763.

[5]Marmur, A. and Rubin, E., "Viscous Effect of Stagnation Depth of Bubbles in a Vertically Oscillating Liquid Column" *Canadian Journal of Chemical Engineering,* Vol. 54, Dec. 1976, pp. 509-514.

[6]Crum, L. A., "Bjerknes' Forces on Bubbles in a Stationary Sound Field," *Journal of the Acoustical Society of America*, Vol. 57, June 1975, pp. 1363-1370.

[7]Hashimoto, H., "Theoretical Studies for Coalescence of Bubbles in Vibrated Liquid Column," *Transactions of JSME*, Ser.B, Vol. 48, June 1982, pp. 1039-1046 (in Japanese).

[8]Pih, H. and Wu, C. G., "Experimental Studies of Vibration of Axially Excited Circular Cylindrical Shells Containing Fluid," *Transactions of ASME*, Ser.B, Vol. 91, Nov. 1969, pp. 1119-1127.

[9]Schoenhals, R. J. and Overcamp, T. J., "Pressure Distribution and Bubble Formation Induced by Longitudinal Vibration of a Flexible Liquid-Filled Cylinder," *Transactions of ASME,* Ser.D, Vol. 89, Dec. 1967, pp. 737-747.

[10]Fritz, C. G., Ponder, C. A. Jr., and Blount, D. H., "Bubble Coalescence in a Longitudinally Vibrated Column," Symposium on Cavitation Liquid in Fluid Machinery, ASME Winter Annual Meeting, Chicago, IL, Nov. 1965, pp. 148-161.

[11]Remenyik, C. J., "Surface Instability of Stationary Air Bubbles," *Proceedings of International Colloquium on Drops and Bubbles,* Vol. 2, Aug. 1974, pp. 592-605.

[12]Iakimov, I. L., "Relation of Drift Effect to Gas Bubble Volume in Vibrated Liquid Column," *Izvestiia Akademii Nauk SSSR, Mekhanika Zhidkostei i Gaza,* No. 4, 1978, pp. 138-140.

[13]Hashimoto, H. and Sudo, S., "Frequency Characteristics of Pressure Induced by Vertical Vibration of a Cylindrical Container Containing Liquid," *Proceedings of the 1982 Joint Conference of Experimental Mechanics,* Hawaii, Pt. 1, May 1982, pp. 353-358.

[14]Minnaert, M., "On Musical Air-Bubbles and the Sounds of Running Water," *Philosophical Magazine*, Vol. 16, 1933, pp. 235-248.

[15]Baird, M. H. I., "Resonant Bubbles in a Vertically Vibrating Liquid Column," *Canadian Journal of Chemical Engineering,* Vol. 41, April 1963, pp. 52-55.

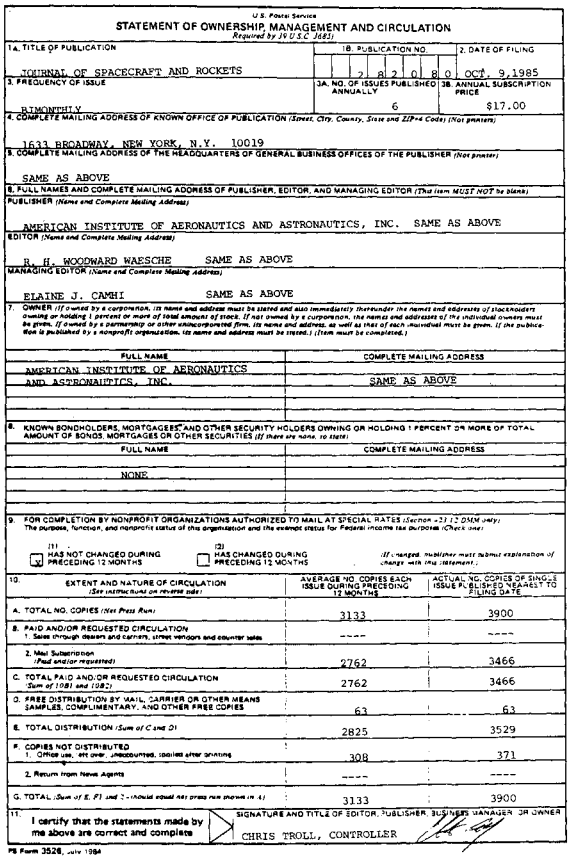

U.S. Postal Service
STATEMENT OF OWNERSHIP, MANAGEMENT AND CIRCULATION
Required by 39 U.S.C. 3685)

1A. TITLE OF PUBLICATION	1B. PUBLICATION NO.	2. DATE OF FILING
JOURNAL OF SPACECRAFT AND ROCKETS	2 8 2 0 8 0	OCT. 9,1985
3. FREQUENCY OF ISSUE	3A. NO. OF ISSUES PUBLISHED ANNUALLY	3B. ANNUAL SUBSCRIPTION PRICE
BIMONTHLY	6	$17.00

4. COMPLETE MAILING ADDRESS OF KNOWN OFFICE OF PUBLICATION (Street, City, County, State and ZIP+4 Code) (Not printers)

1633 BROADWAY, NEW YORK, N.Y. 10019

5. COMPLETE MAILING ADDRESS OF THE HEADQUARTERS OF GENERAL BUSINESS OFFICES OF THE PUBLISHER (Not printer)

SAME AS ABOVE

6. FULL NAMES AND COMPLETE MAILING ADDRESS OF PUBLISHER, EDITOR, AND MANAGING EDITOR (This item MUST NOT be blank)

PUBLISHER (Name and Complete Mailing Address)

AMERICAN INSTITUTE OF AERONAUTICS AND ASTRONAUTICS, INC. SAME AS ABOVE

EDITOR (Name and Complete Mailing Address)

R. H. WOODWARD WAESCHE SAME AS ABOVE

MANAGING EDITOR (Name and Complete Mailing Address)

ELAINE J. CAMHI SAME AS ABOVE

7. OWNER (If owned by a corporation, its name and address must be stated and also immediately thereunder the names and addresses of stockholders owning or holding 1 percent or more of total amount of stock. If not owned by a corporation, the names and addresses of the individual owners must be given. If owned by a partnership or other unincorporated firm, its name and address, as well as that of each individual must be given. If the publication is published by a nonprofit organization, its name and address must be stated.) (Item must be completed.)

FULL NAME	COMPLETE MAILING ADDRESS
AMERICAN INSTITUTE OF AERONAUTICS AND ASTRONAUTICS, INC.	SAME AS ABOVE

8. KNOWN BONDHOLDERS, MORTGAGEES, AND OTHER SECURITY HOLDERS OWNING OR HOLDING 1 PERCENT OR MORE OF TOTAL AMOUNT OF BONDS, MORTGAGES OR OTHER SECURITIES (If there are none, so state)

FULL NAME	COMPLETE MAILING ADDRESS
NONE	

9. FOR COMPLETION BY NONPROFIT ORGANIZATIONS AUTHORIZED TO MAIL AT SPECIAL RATES (Section 423.12 DMM only)
The purpose, function, and nonprofit status of this organization and the exempt status for Federal income tax purposes (Check one)

(1) [X] HAS NOT CHANGED DURING PRECEDING 12 MONTHS (2) [ ] HAS CHANGED DURING PRECEDING 12 MONTHS

(If changed, publisher must submit explanation of change with this statement.)

10. EXTENT AND NATURE OF CIRCULATION (See instructions on reverse side)	AVERAGE NO. COPIES EACH ISSUE DURING PRECEDING 12 MONTHS	ACTUAL NO. COPIES OF SINGLE ISSUE PUBLISHED NEAREST TO FILING DATE
A. TOTAL NO. COPIES (Net Press Run)	3133	3900
B. PAID AND/OR REQUESTED CIRCULATION 1. Sales through dealers and carriers, street vendors and counter sales	----	----
2. Mail Subscription (Paid and/or requested)	2762	3466
C. TOTAL PAID AND/OR REQUESTED CIRCULATION (Sum of 10B1 and 10B2)	2762	3466
D. FREE DISTRIBUTION BY MAIL, CARRIER OR OTHER MEANS SAMPLES, COMPLIMENTARY, AND OTHER FREE COPIES	63	63
E. TOTAL DISTRIBUTION (Sum of C and D)	2825	3529
F. COPIES NOT DISTRIBUTED 1. Office use, left over, unaccounted, spoiled after printing	308	371
2. Return from News Agents	----	----
G. TOTAL (Sum of E, F1 and 2 - should equal net press run shown in 4)	3133	3900

11. I certify that the statements made by me above are correct and complete

SIGNATURE AND TITLE OF EDITOR, PUBLISHER, BUSINESS MANAGER, OR OWNER
CHRIS TROLL, CONTROLLER

PS Form 3526, June 1984